Journal of Applied Sciences

ISSN 1812-5654

science alert

ANSInet
an open access publisher
http://ansinet.com

Journal of Applied Sciences 7 (11): 1467-1474, 2007
ISSN 1812-5654

Study of an Engineering Mixed Contact: Part III- Results for Isosceles Truncated Triangle Surface Ridges

Yongbin Zhang
Zhejiang Jinlei Electronic and Mechanical Co. Ltd., Zhejiang Province, People's Republic of China

Abstracts: It presents the results obtained from the analysis when the isosceles triangle surface ridge is shaved on the top i.e., when the contact surface ridge is isosceles truncated triangle. For the studied contact and surface ridges, the contact stiffness of the whole contact is obtained and compared for different degrees of the shaving of the surface ridge. The load-carrying capacities and contact stiffness of the direct contact between a single ridge and the smooth plane are studied for different surface ridge geometry parameter values. The load partitions in the contact are obtained for different degrees of the surface ridge shaving. The temperature rises on the ridge surface in the direct contact are computed for different degrees of the surface ridge shaving and for wide load ranges carried by the direct contact when the Poisson's ratios, Young's moduli of elasticity and compressive yielding strengths of the contact surfaces are, respectively taken as insensitive to the contact surface temperature rise. These obtained results are compared and the conclusions are drawn concerning the shaving of the contact surface ridge in the present mode of contact.

Key words: Engineering mixed contact, dry contact, oxidized chemical boundary layer, physical adsorbed boundary layer, hydrodynamic contact

INTRODUCTION

Analysis were presented by Zhang (2007a) for an engineering mixed lubrication contact when the contact surface ridges are, respectively isosceles triangle and isosceles truncated triangle. This mode of contact was commented to be more engineering and realistic. Results obtained for it could be of significant interest. Details about this mode of contact were shown in the first part (Zhang, 2007a).

In the second part (Zhang, 2007b), results were presented for this mode of contact obtained from the analysis presented in the first part (Zhang, 2007a) when the contact surface ridge is isosceles triangle. The performance of the modeled contact including its load-carrying capacity and contact stiffness were obtained for the assumed surface ridge profiles.

The present study attempts to study the performance of the modeled contact in the fore two parts (Zhang, 2007a,b) when the isosceles triangle contact surface ridge is shaved on the top in different degrees i.e., when the contact surface ridge is isosceles truncated triangle. Computations are carried out for the contact of this shaved surface ridge profile for chosen operating conditions. Results obtained in these computations are presented and discussed in the following. The present study attempts to explore the influence of the contact surface ridge profile on the performance of the modeled contact.

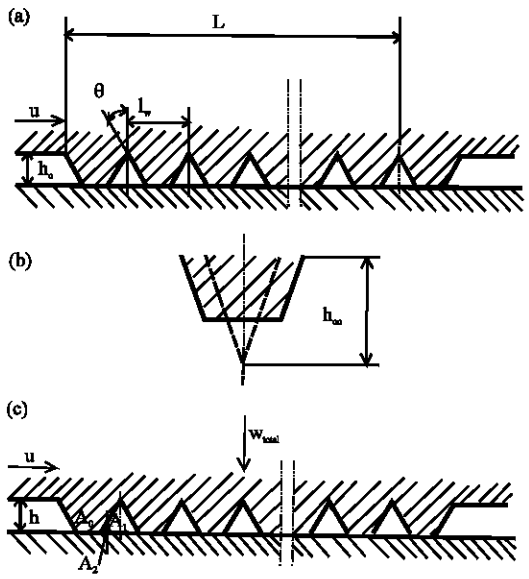

Fig. 1: Studied contact in the present study. (a) The contact model and its ridge geometries, (b) A shaved contact surface ridge profile and its initial height h_{00} before shaving and (c) Picture of the contact under loading

CONTACT MODEL

A general contact modeled in the present study and its surface ridge geometries are shown in Fig. 1a. The

shaved degree of the contact surface ridge in this contact is shown by the value of the original half contact width b_0 of the shaved ridge shown in Fig. 1a. A larger value of the width b_0 of a ridge represents a deeper degree of the shaving of this ridge. Before shaving, the initial height of the (isosceles triangle) surface ridge is assumed as h_{00}. Figure 1b pictures a shaved contact surface ridge profile and its initial height h_{00} before shaving in the present study. Figure 1c pictures the studied contact under loading.

OPERATIONAL PARAMETERS

The values of the operational parameters in the present study are chosen as follows:

$$h_0 = 1.6\mu m, p_y = 0.3GPa, E_a = 193GPa, \nu = 0.28$$
$$\alpha = 23.7GPa^{-1}, \eta_0 = 0.1Pa\cdot s, u = (-)30ms^{-1},$$
$$h_{cr,ncf} = 30nm, f = 0.35, k_m = 40W/(m\cdot{}^\circ C),$$
$$c_m = 400J/(kg\cdot{}^\circ C), \rho_m = 7800kg\,m^{-3}, N = 100$$

These operational parameters were shown in the first part (Zhang, 2007a). The materials of the two contact surfaces are taken as same.

RESULTS

The results obtained from the analysis developed in the first part (Zhang, 2007a) according to the above operational parameter values are demonstrated and discussed as follows when the contact surface ridge is isosceles truncated triangle. The presented parameters in the results are all in dimensionless form. The definitions of these dimensionless parameters are shown in the Nomenclature.

Critical load and interference of elastic deformation of the direct contact between a single ridge and the smooth plane: Figure 2a plots the variations of the dimensionless maximum load $\overline{W}_{max,e}$ carried by the direct contact between a single ridge and the smooth plane in the ridge elastic deformation regime in the present model with the original half contact width of the ridge for different values of the half ridge angle θ. Attention that the dimensionless parameter $\overline{W}_{max,e}$ is defined as

$$\overline{w}_{max,e}(\overline{\overline{b}}_0, \theta) = w_{max,e}(b_0, \theta)/w_{max,e}(0, \theta).$$

It is shown that for a given θ value this variation is linear and the value of $\overline{W}_{max,e}$ is increased with the increase of $\overline{\overline{b}}_0$; This increasing proportionality is greater

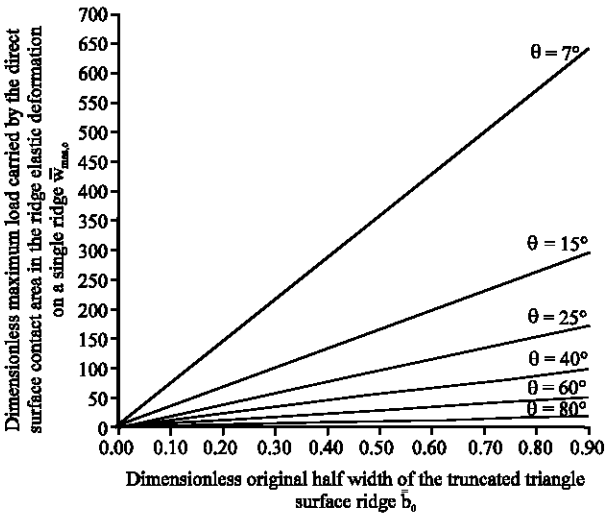

Fig. 2a: Variations of the dimensionless maximum load $\overline{w}_{max,e}$ carried by the direct contact between a single ridge and the smooth plane in the ridge elastic deformation regime with the original half contact width of the ridge for different values of the half ridge angle θ

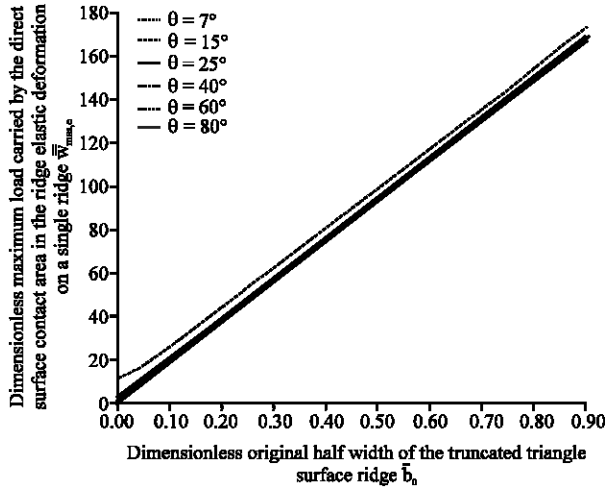

Fig. 2b: Variations of another defined dimensionless maximum load $\overline{\overline{w}}_{max,e}$ carried by the direct contact between a single ridge and the smooth plane in the ridge elastic deformation regime with the original half contact width of the ridge for different θ values

for smaller θ values. For a given $\overline{\overline{b}}_0$ value, the value of $\overline{W}_{max,e}$ is significantly increased with the reduction of the θ value particularly at larger $\overline{\overline{b}}_0$ values. These indicate that the increasing effect of the shaving of the ridge on the load-carrying capacity of the

elastic direct contact between a single ridge and the smooth plane in the present model is greater for smaller θ values. This effect is very significant for large $\bar{\bar{b}}_0$ values i.e., deep degrees of the ridge shaving and for small θ values.

Figure 2b plots the variations of another defined dimensionless maximum load $\bar{w}_{max,e}$ carried by the direct contact between a single ridge and the smooth plane in the ridge elastic deformation regime in the present model with the original half contact width of the ridge for different θ values. Attention that in Fig. 2b the dimensionless load $\bar{w}_{max,e}$ is defined as;

$$\bar{\bar{w}}_{max,e}(\bar{\bar{b}}_0,\theta) = w_{max,e}(b_0,\theta)/w_{max,e}(0,\ 25^\circ)$$

The value of the dimensionless load $\bar{\bar{w}}_{max,e}$ directly reflects its dimensional value i.e., the absolute load value $w_{max,e}$ (b_0,θ). It is shown that for a given θ value the absolute (i.e., dimensional) value of the maximum load carried by the direct contact between a single ridge and the smooth plane in the ridge elastic deformation regime in the present model is linearly and significantly increased with the increase of $\bar{\bar{b}}_0$; This increasing proportionality is same for different θ values; For a given $\bar{\bar{b}}_0$ value this absolute load value is slightly increased with the increase of the value of θ. These indicate that in the case of the shaved contact surface ridge the original half contact width $\bar{\bar{b}}_0$ of the ridge has the most significant effect on the absolute load-carrying capacity of the elastic direct contact between a single ridge and the smooth plane than the other ridge geometry parameters in the present model.

Figure 3 plots the variations of the critical (i.e., maximum) interference $\bar{\Delta}_{cr,e}$ of the elastic direct contact between a single ridge and the smooth plane in the present model with the original half contact width of the ridge for different θ values. It is shown that for a given θ value this critical interference is rapidly reduced with the increase of $\bar{\bar{b}}_0$ when the value of $\bar{\bar{b}}_0$ is small, but is very slightly varied with $\bar{\bar{b}}_0$ when the value of $\bar{\bar{b}}_0$ is relatively large. For a given $\bar{\bar{b}}_0$ value, this critical interference is significantly increased with the increase of the value of θ.

Load-carrying capacity and contact stiffness of the direct contact between a single ridge and the smooth plane: Figure 4a plots the load carried by the direct contact between a single ridge and the smooth plane against the film thickness H for different $\bar{\bar{b}}_0$ values in the present model when the ridge is in elastic deformation and the half ridge angle θ is 25°. It is shown that for a given $\bar{\bar{b}}_0$ value, in the ridge elastic deformation regime this load is rapidly increased with the reduction of the film thickness H particularly for higher $\bar{\bar{b}}_0$ values; For the same film

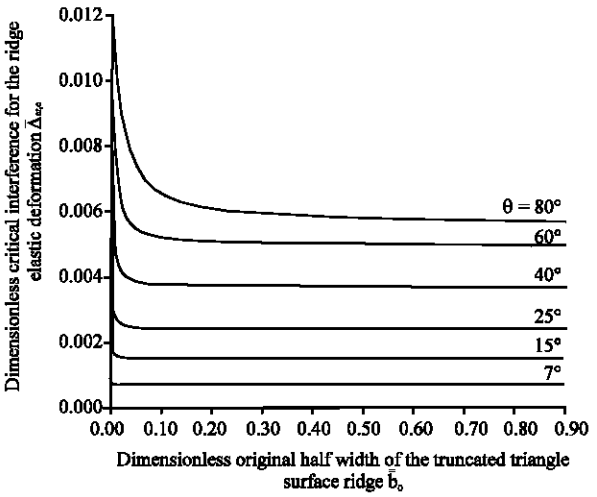

Fig. 3: Variations of the critical (i.e., maximum) interference $\bar{\Delta}_{cr,e}$ of the elastic direct contact between a single ridge and the smooth plane with the original half contact width of the ridge for different θ values

thickness H, in the ridge elastic deformation regime, this load is significantly increased with the increase of $\bar{\bar{b}}_0$ particularly when the value of $\bar{\bar{b}}_0$ is low; This load can reach quite large values for high $\bar{\bar{b}}_0$ model values. These show that is present model the increase of the degree of the shaving of the ridge significantly increases the load-carrying capacity of the elastic direct contact between a single ridge and the smooth plane.

Figure 4b plots the similar curves as in Fig. 4a when the ridge is in plastic deformation and the half ridge angle θ is 25°. It is shown that for a given $\bar{\bar{b}}_0$ value, in the ridge plastic deformation regime the load carried by the direct contact between a single ridge and the smooth plane in the present model is linearly and significantly increased with the reduction of the film thickness $\bar{H}$; This increasing proportionality is same for different $\bar{\bar{b}}_0$ values; When the ridge is in plastic deformation, the load-carrying capacity of the direct contact between a single ridge and the smooth plane is not dependent on the original half contact width of the shaved ridge; The load carried by this direct contact at the inception of the ridge plastic deformation is rapidly and nearly linearly increased with the increase of $\bar{\bar{b}}_0$.

Figure 4c plots another defined dimensionless load $\bar{\bar{w}}_{A0,single}$ carried by the direct contact between a single ridge and the smooth plane in the present model against the interference $\bar{\bar{\delta}}h$ for different θ values when the ridge is in elastic deformation and $\bar{\bar{b}}_0$ = 0.3318. Here, for the purpose of comparison, the

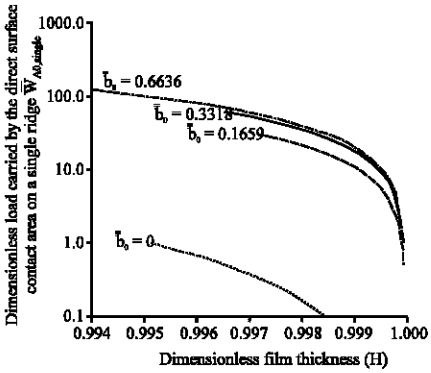

Fig. 4a: Plots of the load carried by the direct contact between a single ridge and the smooth plane against the film thickness H for different $\bar{b}_0$ values when the ridge is in elastic deformation and the half ridge angle θ is 25°

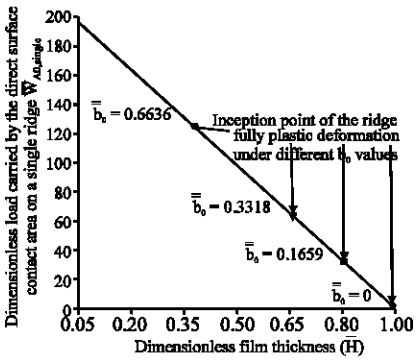

Fig. 4b: Plots of the load carried by the direct contact between a single ridge and the smooth plane against the film thickness $\bar{H}$ for different $\bar{b}_0$ values when the ridge is in plastic deformation and the half ridge angle θ is 25°

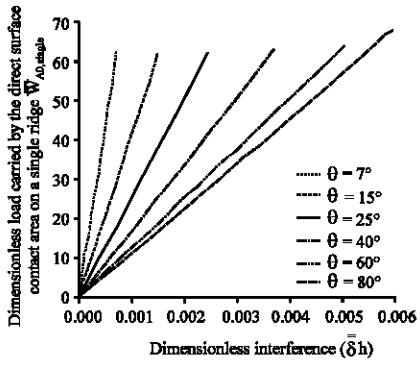

Fig. 4c: Plots of another defined dimensionless load $\bar{w}_{A0,single}$ carried by the direct contact between a single ridge and the smooth plane against the interference $\bar{\delta}\bar{h}$ for different θ values when the ridge is in elastic deformation and $\bar{b}_0$ = 0.3318

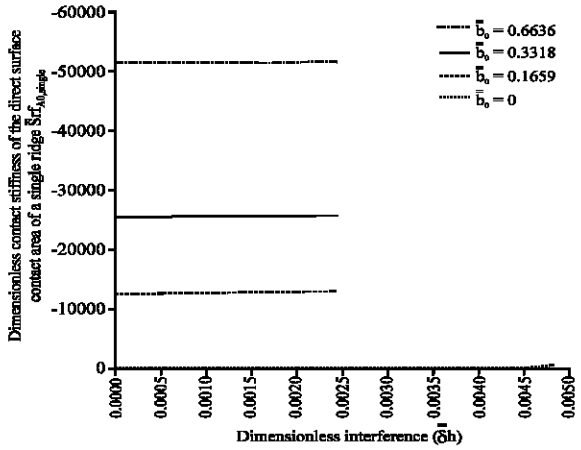

Fig. 5: Plots of the contact stiffness of the direct contact between a single ridge and the smooth plane against the dimensionless interference $\bar{\delta}\bar{h}$ for different $\bar{b}_0$ values when the ridge is in elastic deformation and the half ridge angle θ is 25°

dimensionless load $\bar{w}_{A0,single}$ is defined as:

$$\bar{w}_{A0,single}(\bar{b}_0,\theta) = w_{A0,single}(b_0,\theta)/w_{A0,single}(0,\ 25°)$$

The value of the dimensionless load $\bar{w}_{A0,single}$ directly reflects its dimensional value i.e., the absolute load value $w_{A0,\ single}$ (b_0, θ). It is shown that for a given θ value, in the ridge elastic deformation regime, the absolute value of the load carried by the direct contact between a single ridge and the smooth plane in the present model is linearly and rapidly increased with the increase of the interference $\bar{\delta}\bar{h}$; This increasing proportionality is greater for smaller θ values. In the ridge elastic deformation regime, for a given value of the interference $\bar{\delta}\bar{h}$, this absolute load value is significantly increased with the reduction of the value of the half ridge angle θ particularly for higher values of the interference $\bar{\delta}\bar{h}$. Figure 4c indicates that in the case of the shaved ridge with the same width $\bar{b}_0$, for the same interference $\bar{\delta}\bar{h}$, the reduction of the value of the half ridge angle θ significantly increases the carried load by the direct contact between a single ridge and the smooth plane in the present model when the ridge is in elastic deformation.

Figure 5 plots the contact stiffness of the direct contact between a single ridge and the smooth plane in the present model against the dimensionless interference $\bar{\delta}\bar{h}$ for different $\bar{b}_0$ values when the ridge is in elastic deformation and the half ridge angle θ is 25°. It is shown that for a given $\bar{b}_0$ value, in the ridge elastic deformation regime, the magnitude of this contact stiffness is linearly increased with the increase of the interference $\bar{\delta}\bar{h}$; This increasing proportionality is same for different $\bar{b}_0$ values.

For the same interference $\bar{\bar{\delta}}\bar{\bar{h}}$, in the ridge elastic deformation regime, the magnitude of this contact stiffness is rapidly and nearly linearly increased with the increase of $\bar{\bar{b}}_0$. In the case of the shaved ridge, in the ridge elastic deformation regime, this contact stiffness can be very large and it may mainly depend on the degree of the shaving of the ridge i.e., the value of $\bar{\bar{b}}_0$.

Contact surface temperature rise: Figure 6a plots the temperature rises on the ridge surface in the direct contact between a single ridge and the smooth plane in the present model against the load carried by this contact for different $\bar{\bar{b}}_0$ values when the shaved ridges for the plotted cases are in elastic deformation and the half ridge angle θ is 25°. It is shown that for a given $\bar{\bar{b}}_0$ value, in the ridge elastic deformation regime, this temperature rise is linearly and significantly increased with the increase of the load carried by this direct contact; This increasing proportionality is reduced with the increase of $\bar{\bar{b}}_0$. For the same load carried by this direct contact, in the ridge elastic deformation regime, this temperature rise is significantly reduced with the increase of $\bar{\bar{b}}_0$ particularly when the load carried by this direct contact is heavy. Figure 6a indicates that in the present model, for the same carried load by the direct contact, in the ridge elastic deformation regime, a deeper degree of the shaving of the ridge i.e., a higher value of $\bar{\bar{b}}_0$ significantly reduces the temperature rise on the ridge surface in the direct contact particularly when the load carried by the direct contact is heavy.

Figure 6b plots the temperature rises on the ridge surface in the direct contact between a single ridge and the smooth plane in the present model against the load carried by this contact for different $\bar{\bar{b}}_0$ values and for heavier carried loads by this contact than in Fig. 6a when the half ridge angle θ is 25°. The nearly overlaid curves for different $\bar{\bar{b}}_0$ values shown in Fig. 6b are due to the ridge plastic deformations on these curves for these $\bar{\bar{b}}_0$ values. When the ridge is in plastic deformation, theory shows that the plotted temperature rise in Fig. 6b is not changed by the original half contact width $\bar{\bar{b}}_0$ of the shaved ridge. The minor differences of the curves for different $\bar{\bar{b}}_0$ values in the ridge plastic deformation regime shown in Fig. 6b are due to the computation errors. Figure 6b indicates that when the ridge is in plastic deformation, the temperature rise on the ridge surface in the direct contact in the present model is independent on the value of $\bar{\bar{b}}_0$ i.e., the degree of the shaving of the ridge.

Load partition in the contact: Figure 7a and b plot the ratios R_w of the carried load by the lubricant film lubricated area to that by the whole contact against the

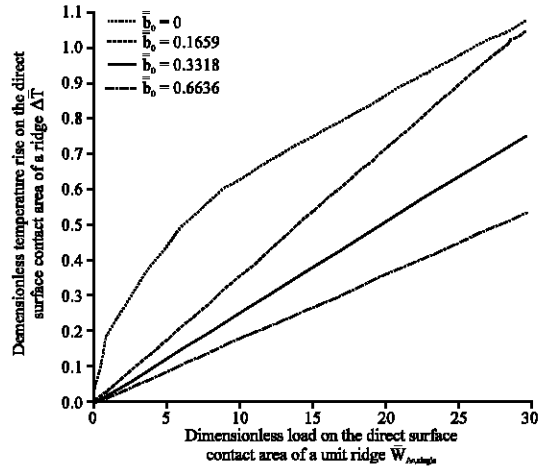

Fig. 6a: Plots of the temperature rises on the ridge surface in the direct contact between a single ridge and the smooth plane against the load carried by this contact for different $\bar{\bar{b}}_0$ values when the shaved ridges for the plotted cases are in elastic deformation and the half ridge angle θ is 25°

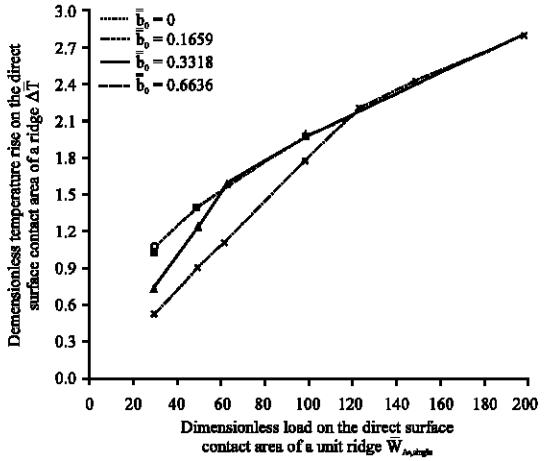

Fig. 6b: Plots of the temperature rises on the ridge surface in the direct contact between a single ridge and the smooth plane against the load carried by this contact for different $\bar{\bar{b}}_0$ values and for heavier carried loads by this contact than in Fig. 6a when the half ridge angle θ is 25°

film thickness H for different $\bar{\bar{b}}_0$ values in the present contact when the half ridge angle θ is 25°. Figure 7a shows that for the shaved ridge i.e., for a given $\bar{\bar{b}}_0$ value, the value of R_w is drastically reduced with the reduction of the film thickness H in the present model even when the value of the film thickness H is very close to 1.0; In this case, the value of R_w can be no more than 10% even when the value of H is 0.999. For the same H value, the increase

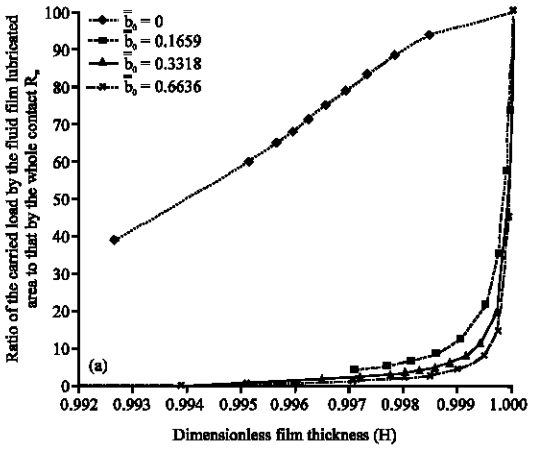

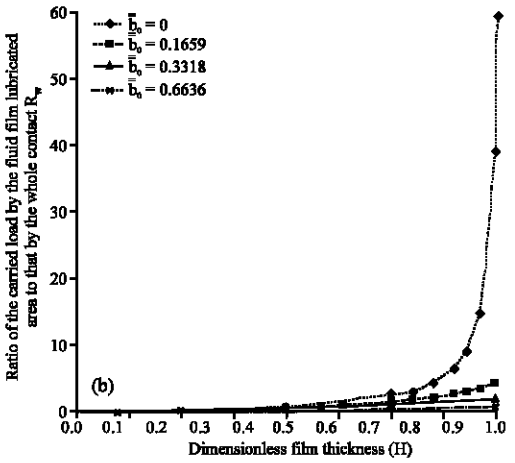

Fig. 7: Plots of the ratio R_w of the carried load by the lubricant film lubricated area to that by the whole contact against the film thickness H for different $\bar{\bar{b}}_0$ values when the half ridge angle θ is 25°

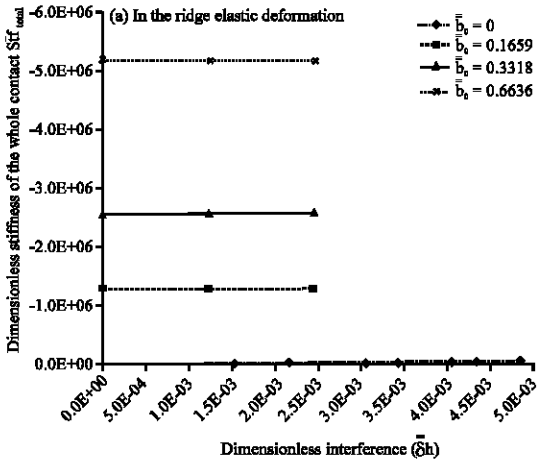

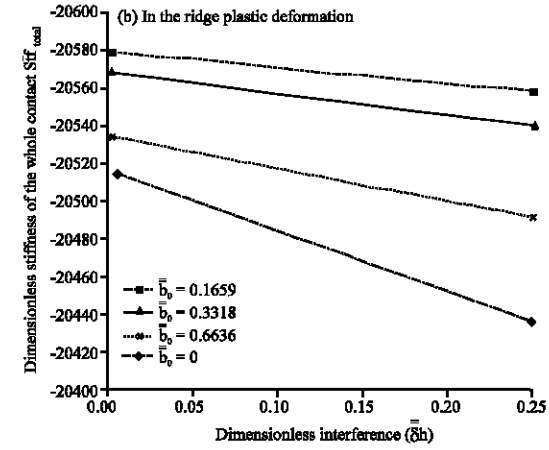

Fig. 8: Variations of the stiffness of the whole contact with the interference $\bar{\bar{\delta}}\bar{h}$ for different $\bar{\bar{b}}_0$ values when the half ridge angle θ is 25°

of $\bar{\bar{b}}_0$ very significantly reduces the value of R_w in the present model particularly for relatively small $\bar{\bar{b}}_0$ values and for the value of the film thickness H approaching 1.0. Figure 7a indicates that for the same H value, the shaving of the ridge practically largely reduces the value of R_w and makes the direct contact mainly carry the load of the whole contact in the present model. For the shaved ridge, the performance of the contact in the present model may practically be determined by the performance of the direct contact between the contact surfaces according to the values of R_w plotted in Fig. 7a. This determination is heavier for a deeper degree of the shaving of the ridge.

Figure 7b indicates that in the present model, when the value of the film thickness H is a bit lower than 1.0, a practical shaving of the ridge reduces the value of R_w to no more than 5% and makes the direct contact between the contact surfaces carry almost all the load of the whole contact. In this case, the performance of the contact in the present model is surely determined by the performance of the direct contact between the contact surfaces. Figure 7a and b indicate that for the same H value a practical shaving of the ridge makes the direct contact between the contact surfaces carry much more portion of the load of the whole contact and much more determine the performance of the whole contact in the present model compared to the case of no ridge shaving.

Stiffness of the whole contact: Figure 8a plots the variations of the stiffness of the whole contact with the interference $\bar{\bar{\delta}}\bar{h}$ for different $\bar{\bar{b}}_0$ values when the ridge is in elastic deformation and the half ridge angle θ is 25°. These variations are very similar with the variations of the contact stiffness of the direct contact between a single ridge and the smooth plane with the interference $\bar{\bar{\delta}}\bar{h}$ for the same $\bar{\bar{b}}_0$ values plotted in Fig. 5.

For a given $\bar{\bar{b}}_0$ value, in the ridge elastic deformation regime, the magnitude of the stiffness of the whole contact is linearly increased with the increase of the interference $\bar{\bar{\delta}}\bar{\bar{h}}$ in the present model. This increasing proportionality is same for different $\bar{\bar{b}}_0$ values. For the same interference $\bar{\bar{\delta}}\bar{\bar{h}}$, in the ridge elastic deformation regime, the magnitude of the stiffness of the whole contact is rapidly and nearly linearly increased with the increase of $\bar{\bar{\delta}}\bar{\bar{h}}$ in the present model. In the case of the shaved ridge, in the ridge elastic deformation regime, this contact stiffness can be very large and it may mainly depend on the degree of the shaving of the ridge i.e., the value of $\bar{\bar{b}}_0$.

Figure 8b plots the variations of the stiffness of the whole contact with the interference $\bar{\bar{\delta}}\bar{\bar{h}}$ for different $\bar{\bar{b}}_0$ values in the present model when the ridge is in plastic deformation and the half ridge angle θ is 25°. It is shown that in the ridge plastic deformation regime, the magnitudes of this contact stiffness are close for all the $\bar{\bar{\delta}}\bar{\bar{h}}$ and $\bar{\bar{b}}_0$ values and they are much lower than the magnitudes of this contact stiffness for the same $\bar{\bar{b}}_0$ values in the case of the shaved ridge when the ridge is in elastic deformation as plotted in Fig. 8a.

CONCLUSIONS

The current study presents the results obtained from the analysis developed in Zhang (2007a) for an engineering mixed lubrication contact when the contact surface ridge is isosceles truncated triangle. The modeled contact is one-dimensional composed of a rough plane and another ideally smooth plane. On the rough plane is periodically imposed isosceles truncated triangle ridges. The rough plane is taken as elastic-plastic and moving, while the ideally smooth plane is taken as rigid and stationary. In the modeled contact, the direct contact occurs between the tip of the ridge and the smooth plane, while between other parts of the ridge and the smooth plane, respectively occur the conventional hydrodynamic lubricated contact and the physical adsorbed boundary layer contact according to the lubricating film thickness formed between these mated contact surfaces.

The obtained results in the present study indicate that in the present contact the increasing effect of the shaving of the ridge on the load-carrying capacity of the elastic direct contact between a single ridge and the smooth plane is greater for smaller values of the half ridge angle θ; This effect is very significant for deep degrees of the ridge shaving and for small θ values; In the case of the shaved contact surface ridge the original half contact width $\bar{\bar{b}}_0$ of the ridge has the most significant effect on the absolute load-carrying capacity of the elastic direct contact between a single ridge and the smooth plane than the other ridge geometry parameters; The increase of the degree of the shaving of the ridge significantly increases the load-carrying capacity of this direct contact. When the ridge is in plastic deformation, the load-carrying capacity of the direct contact between a single ridge and the smooth plane is independent on the original half contact width of the shaved ridge; The load carried by this direct contact at the inception of the ridge plastic deformation is rapidly and nearly linearly increased with the increase of $\bar{\bar{b}}_0$. In the case of the shaved ridge, in the ridge elastic deformation regime, the contact stiffness of the direct contact between a single ridge and the smooth plane and the whole contact both can be very large and they may mainly depend on the degree of the shaving of the ridge.

For the same carried load by the direct contact, in the ridge elastic deformation regime, a deeper degree of the shaving of the ridge significantly reduces the temperature rise on the ridge surface in the direct contact particularly when the load carried by the direct contact is heavy. While, in the ridge plastic deformation regime, the temperature rise on the ridge surface in the direct contact is independent on the degree of the shaving of the ridge.

For the same separation between the two planes, a practical shaving of the ridge makes the direct contact between the two planes carry much more portion of the load of the whole contact and much more determine the performance of the whole contact compared to the case of no ridge shaving.

NOMENCLATURE

b_0 = Original half contact width of the shaved ridge, shown in Fig. 1a

$\bar{\bar{b}}_0$ = b_0/h_{00}

c_m = Specific heat of the rough surface

E_a = Young's module of elasticity of the contact surface

f = Friction coefficient of the ridge-plane direct contact area

h = Film thickness between the root of the ridge and the smooth plane

h_0 = Initial height of the truncated triangle surface ridge

h_{00} = Initial height of the (isosceles triangle) surface ridge before shaving

$\bar{H}$ = Dimensionless film thickness, h/h_0

$\bar{\bar{H}}$ = Universally normalized film thickness, h/h_{00}

k_m = Heat conduction coefficient of the rough surface

N = Number of the surface ridge in the whole contact

p_y = Compressive yielding strength of the ridge
R_w = Ratio of the carried load by the lubricant film lubricated area to that by the whole contact in the present modeled contact
$\bar{S}tf$ = Dimensionless stiffness, $d\bar{w}/d\bar{H}$
T_a = Ambient temperature, 20°C
u = Sliding speed between the contact surfaces
w = Dimensional load per unit contact length
$w_{max,e}$ = Maximum load on the direct surface contact area between a single ridge and the smooth plane when the ridge undergoes elastic deformation
$\bar{w}$ = Dimensionless load, $w/w_{max,e}$
$\bar{\bar{w}}$ = Universally normalized load, $w/w_{max,e}(0,25°)$

$$\bar{w}_{max,e}(\bar{b}_0,\theta) = w_{max,e}(b_0,\theta)/w_{max,e}(0,\theta)$$

$$\bar{\bar{w}}_{max,e}(\bar{\bar{b}}_0,\theta) = w_{max,e}(b_0,\theta)/w_{max,e}(0,\ 25°)$$

v = Poisson's ratio of the contact surface
θ = Half ridge angle
η_0 = Viscosity of continuum lubricant at ambient condition
α = Viscosity-pressure index of lubricant
ρ_m = Density of the rough surface
ΔT = Dimensional temperature rise of the direct contact area between the ridge and the smooth plane
$\Delta\bar{T}$ = Dimensionless temperature rise, $\Delta T/T_a$
δh = Dimensional interference of the direct contact between a single ridge and the smooth plane, h_0-h
$\bar{\bar{\delta h}}$ = $\delta h/h_{00}$
$\Delta_{cr,e}$ = Dimensional critical (i.e., maximum) interference of the elastic direct contact between a single ridge and the smooth plane
$\bar{\Delta}_{cr,e}$ = $\Delta_{cr,e}/h_{00}$

SUBSCRIPTS

A_0 = On the direct surface contact area
single = Between a single ridge and the smooth plane
total = Of the whole contact in the present model

REFERENCES

Zhang, Y.B., 2007a. Study of an engineering mixed contact: Part I- Theoretical analysis. J. Applied Sci., (Submitted).

Zhang, Y.B., 2007b. Study of an engineering mixed contact: Part II- Results for isosceles triangle surface ridges. J. Applied Sci., (Submitted).